Showcasing research from Professor Tulchinsky's laboratory, Institute of Chemistry, Hebrew University of Jerusalem, Israel.

Sulfonium cations as versatile strongly π-acidic ligands

While the discovery of tunable π-acidic ligands has opened new opportunities in catalysis, the coordination of sulfonium cations, although isoelectronic to tertiary phosphines, has been neglected. Here we present complexes of aliphatic and aromatic sulfonium stabilized by pincer frameworks and exhibiting short M-S bonds. Computational studies of these unusual complexes revealed that π back-donation is the dominant L-M bonding interaction, which places these sulfonium ligands among the best π-acceptors available. In the picture, the sulfonium cation "quenches its thirst" by drinking electron density from the metal held by phosphine arms.

As featured in:

See Yuri Tulchinsky *et al.*, *Chem. Sci.*, 2022, **13**, 4770.

ROYAL SOCIETY OF CHEMISTRY

rsc.li/chemical-science

Registered charity number: 207890

Chemical Science

ROYAL SOCIETY OF CHEMISTRY

EDGE ARTICLE

View Article Online
View Journal | View Issue

Check for updates

Cite this: *Chem. Sci.*, 2022, **13**, 4770

All publication charges for this article have been paid for by the Royal Society of Chemistry

Received 29th January 2022
Accepted 14th March 2022

DOI: 10.1039/d2sc00588c

rsc.li/chemical-science

Open Access Article. Published on 14 March 2022. Downloaded on 2/9/2026 9:09:14 AM.
This article is licensed under a Creative Commons Attribution 3.0 Unported Licence.

Sulfonium cations as versatile strongly π-acidic ligands†

Ruiping Li, Nitsan Barel, Vasudevan Subramaniyan, Orit Cohen, Françoise Tibika and Yuri Tulchinsky *

More than a century old, sulfonium cations are still intriguing species in the landscape of organic chemistry. On one hand they have found broad applications in organic synthesis and materials science, but on the other hand, while isoelectronic to the ubiquitous tertiary phosphine ligands, their own coordination chemistry has been neglected for the last three decades. Here we report the synthesis and full characterization of the first Rh(I) and Pt(II) complexes of sulfonium. Moreover, for the first time, coordination of an aromatic sulfonium has been established. A thorough computational analysis of the exceptionally short S–Rh bonds obtained attests to the strongly π-accepting nature of sulfonium cations and places them among the best π-acceptor ligands available today. Our calculations also show that embedding within a pincer framework enhances their π-acidity even further. Therefore, in addition to the stability and modularity that these frameworks offer, our pincer complexes might open the way for sulfonium cations to become powerful tools in π-acid catalysis.

Introduction

Rethinking the coordination chemistry of main group elements has often led to breakthroughs in metal-based homogeneous catalysis. For instance, extending the chemistry of B, Al, Ga, Sn, and Bi gave birth to the concept of σ-acceptor (aka Z-type) ligands.[1] Peters,[2] Lu[3] and others[4] have used complexes of these ligands for such fundamentally important processes as N_2 fixation, CO_2 reduction, and H_2 activation.

The electron-withdrawing nature of Z-type ligands also offered new opportunities for π-acid catalysis, as demonstrated by Inagaki with borane-based pincer ligands,[5] and Gabbai with ligands based on antimony,[6] and carbenium cations.[7] On the other hand, a significant advance in π-acid catalysis was achieved by Alcarazo by stretching the π-acceptor properties of phosphine[8] and arsine[9] to the extreme through the introduction of positively charged substituents.

While seeking to unravel new facets of main group chemistry, the coordination properties of another main-group species, sulfonium cations, have been greatly overlooked. Yet, sulfonium salts are at the forefront of fundamental and applied research due to their countless applications as precursors for sulfur ylides,[10] alkyl and aryl group sources in cross-coupling reactions,[11] photoacids,[12] and many others.[13]

Compared to isoelectronic and isostructural tertiary phosphines, sulfonium cations have their lone pair stabilized by their positive charge, while their low-lying S–C σ*-orbitals become available for accepting electron density. Therefore, together with sulfoxonium, they have attracted attention as non-metal Lewis acids[14] and have been utilized as such for catalysis and anion sensing.[15] However, while tertiary phosphines are perhaps the most iconic family of ligands, only three crystallographically characterized sulfonium complexes of Mo(0) and Mn(I) were reported decades ago (Chart 1a), where these ligands exhibited strongly π-acidic character.[16] Yet, no sulfonium complexes relevant to catalysis have ever been reported, even though formation of transient metal-coordinated

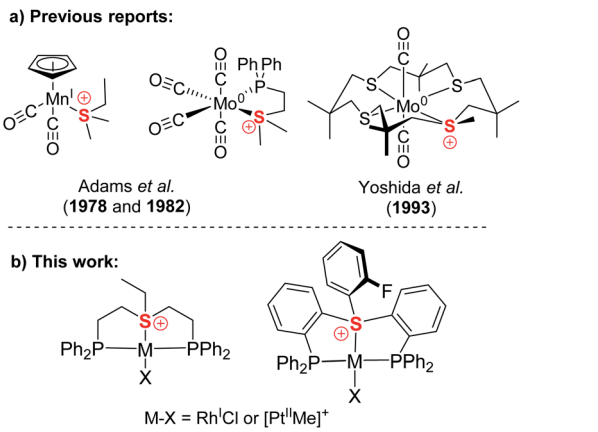

Chart 1 Previously reported sulfonium complexes (a) compared to the pincer type sulfonium complexes presented in the work (b).

Institute of Chemistry, The Hebrew University of Jerusalem, Jerusalem, 9190401, Israel. E-mail: yuri.tulchinsky@mail.huji.ac.il

† Electronic supplementary information (ESI) available. CCDC 2119886–2119894. For ESI and crystallographic data in CIF or other electronic format see DOI: 10.1039/d2sc00588c

© 2022 The Author(s). Published by the Royal Society of Chemistry

Open Access Article. Published on 14 March 2022. Downloaded on 2/9/2026 9:09:14 AM.
This article is licensed under a Creative Commons Attribution 3.0 Unported Licence.

sulfonium intermediates during Pd catalyzed cross-coupling reactions of sulfonium salts has been suggested.[11a]

Here we report the first synthesis and characterization of a series of complexes of both aliphatic and aromatic sulfonium cations with Rh(I) and Pt(II), two representatives of the Pt metal group,[17] which lies at the core of today's homogeneous catalysis (Chart 1b). Our in-depth theoretical analysis of sulfonium–metal interaction demonstrated it to be dominated by π-back bonding. This strongly π-acidic character is further enhanced by the pincer frameworks, which also provide our complexes with structural robustness and modularity, both properties of pivotal importance in catalysis.[18]

Results and discussion

Ligand design and synthesis

Obviously, coordination of the sulfonium cation is hindered by an electrostatic repulsion between its positive charge and that of a metal center (even if partial). So far, the preparation of sulfonium complexes has been achieved by alkylation of the corresponding sulfide complexes. We adopted here a more systematic approach, where the aliphatic or aromatic sulfonium moieties were incorporated within pincer frameworks (**I** and **II**, respectively in Chart 2), bearing chelating phosphine arms. A similar strategy was used earlier by Gandelman to achieve coordination of the nitrenium cation.[19]

We designed aliphatic and aromatic sulfonium ligands with NMR active nuclei in the vicinity of sulfur, namely methylene protons in **I** and a fluorine atom in **II** (Chart 2), that would allow detecting the formation of an S–M bond in solution, by tracing their chemical shifts and magnetic coupling to NMR-active metal centers, ^{103}Rh and ^{195}Pt.

Both sulfonium pincer ligands were prepared by alkylation or arylation of the corresponding bis-phosphine sulfide ligands[20] with the phosphines protected as borane adducts or phosphine oxides in aliphatic and aromatic systems, respectively (Scheme 1), resulting after deprotection in ligands **4a**[OTf] and **4b**[OTf]. To obtain XRD structures of sulfonium ligands (Fig. 1) or their complexes (Fig. 3 and 4, *vide infra*) the triflate counterions were in some cases exchanged for tetraphenylborate or hexafluorophosphate.

Synthesis and characterization of the Rh(I)–sulfonium complexes

The coordinative behavior of the aliphatic sulfonium ligand **4a**[OTf] towards Rh(I) was tested by reacting it with $[RhCl(COE)_2]_2$

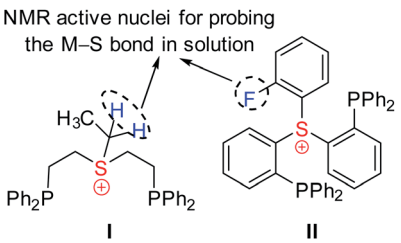

Chart 2 Design of sulfonium-based pincer ligands.

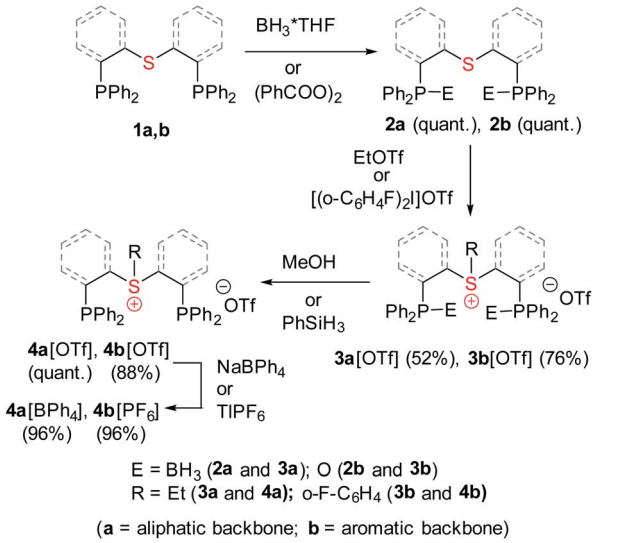

Scheme 1 Synthesis of aliphatic and aromatic sulfonium pincer ligands.

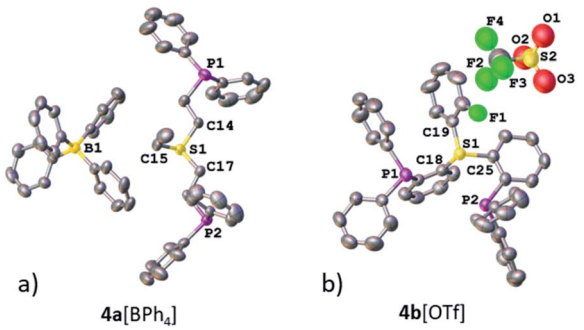

Fig. 1 XRD structures of ligands **4a**[BPh_4] (a) and **4b**[OTf] (b). Co-crystallized solvent molecules and hydrogen atoms are omitted for clarity.

(Scheme 2). A full conversion to a symmetric Rh(I) complex was evident by ^{31}P NMR, as the chemical shift moved from a singlet at −18.2 ppm to a doublet at +46.6 ppm ($^1J_{Rh-P}$ = 127.8 Hz).

In the ^{1}H NMR spectrum, significant downfield shifts of all aliphatic signals are observed (Fig. 2). Each of the methylene protons signals **a** and **b** divides upon coordination into two (**a**** and **b**** pairs, respectively), indicating the formation of a rigid structure with no rotation around C–C bonds. Furthermore, an additional splitting of 1.3 Hz appears in the quartet assigned to the ethyl tail methylene protons (**c****). By means of ^{1}H–^{103}Rh HMBC (Fig. S3†), this splitting has been attributed to a through-bond $^3J_{Rh-H}$ interaction. The latter is only possible if sulfonium is coordinated to the Rh center.

Encouraged by these results, we then turned to the aromatic ligand **4b**[OTf] (Scheme 2). Here also, a full conversion of the ligand to a symmetric Rh(I) complex **5b**[OTf] was evident from the ^{31}P NMR spectrum, where the chemical shift changed from a singlet at −13.0 ppm to a doublet of doublets at +48.7 ppm ($^1J_{Rh-P}$ = 126.0 Hz; $^5J_{F-P}$ = 6.0 Hz). Interestingly, the ^{31}P–^{19}F

© 2022 The Author(s). Published by the Royal Society of Chemistry

Open Access Article. Published on 14 March 2022. Downloaded on 2/9/2026 9:09:14 AM.
This article is licensed under a Creative Commons Attribution 3.0 Unported Licence.

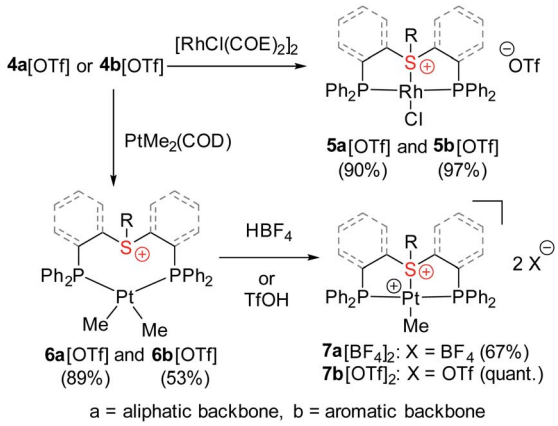

Scheme 2 Synthesis of the Rh(I) and Pt(II)–sulfonium complexes.

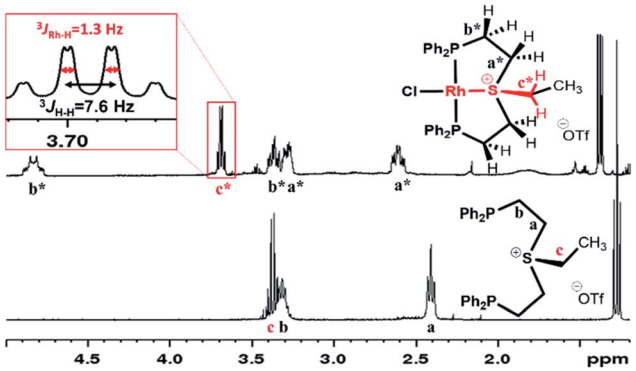

Fig. 2 Aliphatic region of ^{1}H NMR spectra of **4a**[OTf] and **5a**[OTf] in CD_2Cl_2.

interaction unobservable in the spectrum of the free ligand became noticeable after coordination, perhaps due to the additional rigidity of the formed complex.

The ^{19}F NMR spectrum of **5b**[OTf] showed only a small downfield shift compared to the free ligand (−104.1 *vs.* −105.3 ppm, respectively) and no additional splitting by ^{103}Rh could be identified. Likewise, no ^{19}F–^{103}Rh interactions could be detected by HMBC, hence in this case, metal coordination to the aromatic sulfonium moiety could not be validated by NMR alone.

Nevertheless, the irrefutable evidence of sulfonium–Rh bonding in both systems was provided by XRD. Both complexes

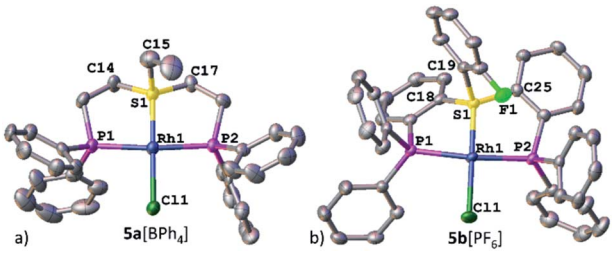

Fig. 3 XRD structures of Rh(I)–sulfonium complexes, **5a**[BPh_4] (a) and **5b**[PF_6] (b). Co-crystallized solvent molecules, counter anions, and hydrogen atoms are omitted for clarity.

5a[BPh_4] and **5b**[PF_6] exhibited a slightly distorted square-planar geometry around the metal (with a τ parameter of 0.1, Table 1), typical of d^8 complexes (Fig. 3a and b, respectively). Notably, the sulfonium–Rh(I) bond lengths of 2.126(2) and 2.112(1) Å observed in **5a**[BPh_4] and **5b**[PF_6], respectively, are among the shortest reported S–Rh bonds (Table 1). These are significantly shorter than in Rh(I) complexes with sulfides (>2.24 Å) and even with sulfoxides (typically, 2.159–2.291 Å).[21] In fact, shorter Rh(I)–S bonds (2.069–2.100 Å) were only observed with the strongest π-acceptor ligands: SO_2 [22] and the related *N*-sulfinylaniline.[23] These exceptionally short S–Rh bonds in **5a**[BPh_4] and **5b**[PF_6] cannot be explained solely by the grip of the pincer framework. Indeed, in both the analogous aliphatic sulfoxide pincer complex **8** that we prepared for comparison (Fig. S17†) and the reported aromatic ones,[24] the Rh–S bonds are still longer than in their sulfonium counterparts (2.135 and 2.134 Å, respectively).

Undoubtedly, these structures not only broaden the very limited pool of known sulfonium complexes but also proved for the first time the coordinating ability of an aromatic sulfonium cation. It is noteworthy, that unlike the α-cationic sulfides, which undergo oxidative addition with electron rich metals,[25] the sulfonium complexes **5a**[OTf] and **5b**[OTf] remained stable as solids and in solutions.

Synthesis and characterization of the Pt(II)–sulfonium complexes

Having shown that stable complexes of sulfonium cations with the neutral RhCl fragment can be obtained, we wondered whether, similarly to cationic nitrenium[19b] and arenium[26] pincer ligands, our frameworks could also induce bonding between these cations and a net positively charged metal

Table 1 Selected bond lengths and angles and geometry indices of complexes

	Complex	S–M bond length (Å)	Rh–Cl or Pt–Me bond length (Å)	Average M–P bond length (Å)	S–M–X and P–M–P angles (°)	Geometry index (τ_4)
Rh–Cl	**5a**[BPh_4]	2.126(2)	2.340(2)	2.296(2)	179.44(9), 164.80(9)	0.11
	5b[PF_6]	2.112(1)	2.324(1)	2.295(1)	178.8(1), 166.0(1)	0.10
	8	2.135(1)	2.369(1)	2.313(1)	172.4(1), 161.2(1)	0.18
Pt–Me	**7a**[BF_4]$_2$	2.258(1)	2.073(5)	2.304(1)	177.8(2), 167.3(1)	0.10
	7b[NTf_2]$_2$	2.261(1)	2.060(4)	2.292(1)	178.7(2), 165.0(1)	0.11
	9[BF_4]	2.336(2)	2.087(7)	2.278(2)	177.6(3), 168.8(1)	0.10

© 2022 The Author(s). Published by the Royal Society of Chemistry

Open Access Article. Published on 14 March 2022. Downloaded on 2/9/2026 9:09:14 AM. This article is licensed under a Creative Commons Attribution 3.0 Unported Licence.

fragment, such as $[PtMe]^+$. To achieve that, we first treated ligands **4a**[OTf] and **4b**[OTf] with $Pt(COD)Me_2$ which resulted in coordination products (Scheme 2), as evident from their ^{31}P NMR spectrum that exhibited downfield shifted peaks at 11.3 or 16.6 ppm with the characteristic ^{195}Pt satellites ($^1J_{Pt-P} = 1813$ and 1781 Hz, respectively). The ^1H NMR signals at 0.42 and 0.65 ppm were assigned to the methyl protons, confirming the formation of $PtMe_2$ complexes **6a**[OTf] and **6b**[OTf], respectively. Moreover, these signals appeared as doublets of doublets due to splitting by two magnetically inequivalent P atoms, a configuration only possible when methyl groups are oriented *cis* to each other (Fig. S1 and S2†). The neutral $PtMe_2$ fragment in **6a**[OTf] and **6b**[OTf] was then transformed into a cation by protonolysis (by HBF_4*OEt_2 or HOTf) resulting in the clean formation of complexes **7a**$[BF_4]_2$ and **7b**$[OTf]_2$ (Scheme 2), as attested by new peaks at 42.4 ($^1J_{Pt-P} = 2736$ Hz) and 44.3 ($^1J_{Pt-P} = 2768$ Hz) ppm, respectively, in ^{31}P NMR. In the aromatic complex **7b**$[OTf]_2$, the ^{31}P NMR signals were much sharper than in **6b**[OTf], and similarly to the Rh(I) complex **5b**[OTf], splitting due to the ^{31}P–^{19}F coupling ($^5J_{P-F} = 3.3$ Hz) became observable.

Unlike complexes **6a**[OTf] and **6b**[OTf], in both **7a**$[BF_4]_2$ and **7b**$[OTf]_2$, the ^1H NMR signals at 1.20 and 1.56 ppm, corresponding to single methyls, appeared as triplets indicating magnetic equivalence of the two phosphines, which is only possible in a mutual *trans*-orientation (Fig. S1 and S2†). Moreover, the signals of the aliphatic protons in **7a**$[BF_4]_2$ followed a pattern similar to that of **5a**[OTf] (Fig. 2), suggesting an analogous structure (Fig. S1†). To further study sulfonium–Pt interaction in solution we applied ^1H–^{195}Pt HMBC, once again focusing on magnetic interaction between Pt and the methylene protons of the ethyl tail (Fig. S4†). While in **6a**[OTf], this coupling constant is negligible (0.2 Hz, presumably due to $^6J_{Pt-H}$), in **7a**$[BF_4]_2$ it reaches 7.7 Hz (most likely, due to $^3J_{Pt-H}$), suggesting the presence of a S–Pt bond in **7a**$[BF_4]_2$, but not in **6a**[OTf]. A similar conclusion about S–Pt bonding in **6b**[OTf] and **7b**$[OTf]_2$ could be drawn by comparing their ^{19}F–^{195}Pt HMBC spectra (Fig. S5†), even though both complexes exhibited nearly identical chemical shifts in ^{19}F NMR (−102.3 and −102.5 ppm, respectively). The former showed no ^{19}F–^{195}Pt correlation, while the latter revealed a prominent cross-peak with a coupling constant of 3.3 Hz, supporting the presence of a sulfonium–Pt bond.

Ultimately, the solid-state structures of **6a**$[BPh_4]$, **7a**$[BF_4]_2$, and **7b**$[NTf_2]_2$ (the latter was prepared by treating **6b**[OTf] with an excess of bistriflimide) were established by single crystal XRD (Fig. 4c, a and b, respectively). In **6a**$[BPh_4]$, as expected from the NMR analysis, no Pt–S bond was observed, and the methyl groups indeed exhibited a *cis* configuration. In contrast, both **7a**$[BF_4]_2$ and **7b**$[NTf_2]_2$ exhibited Pt–S bonds of 2.258(1) and 2.261(1) Å, respectively (see Table 1). Surprisingly, despite electrostatic repulsion between the cationic sulfonium and the $[PtMe]^+$ fragment, the Pt–S bond in **7a**$[BF_4]_2$ is shorter than that in its neutral sulfide analog **9**$[BF_4]$, 2.336(2) Å, prepared for comparison (Fig. 4d).

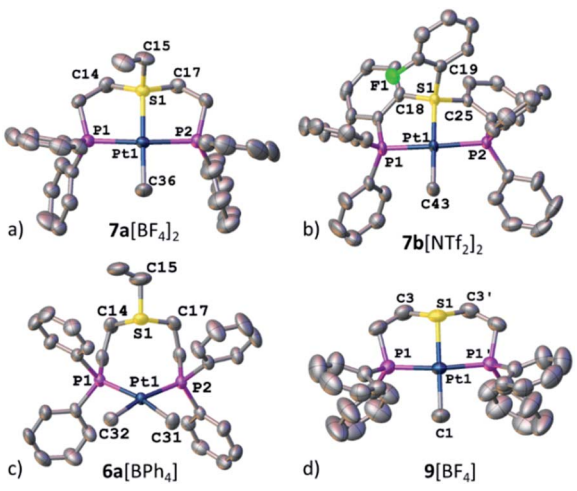

Fig. 4 XRD structures of Pt(II) complexes, **7a**$[BF_4]_2$ (a), **7b**$[NTf_2]_2$ (b), **6a**$[BPh_4]$ (c), and **9**$[BF_4]$ (d). Co-crystallized solvent molecules, counter anions, and hydrogen atoms are omitted for clarity.

Theoretical analysis of metal–sulfonium bonding and the influence of the pincer framework

The exceptionally short metal–sulfonium bonds observed in our Rh complexes prompted us to undertake a computational investigation by DFT. To gain a proper insight, we applied the energy decomposition analysis[27] combined with the natural orbitals for chemical valence theory (EDA-NOCV) which provides a quantitative description of L–M bonding in a visual and chemically intuitive manner.[28,29] In this method the overall interaction energy (ΔE_{int}) between two molecular fragments (*e.g.* the sulfonium ligand and the rest of the complex) is assessed by means of EDA; then NOCV is applied to extract the total orbital interaction contribution (ΔE_{orb}) and decompose it into individual constituents ($\Delta E_{orb(n)}$) according to their orbital symmetry. Each such constituent is then represented by a deformation density plot ($\Delta\rho_{(n)}$) that visualizes the redistribution of charge upon combination of the two molecular fragments.

First, we considered the Rh–S bonding interactions in the model monodentate aliphatic and aromatic sulfonium complexes **10a** and **10b** and compared them with analogous complexes of neutral phosphines, sulfides and sulfoxides, as well as with a few representative cationic ligands. By inspecting the deformation density plots of the most significant orbital interactions ($\Delta E_{orb(n)}$), we could identify a single σ-symmetric interaction that has a clear L → M donation character, and two π-symmetric ones (perpendicular and parallel to the coordination plane) corresponding to the M → L back-donation (see representative deformation density maps of **10a** in Fig. 5a and for other maps see Tables S22 and S23†). Interestingly, in the only reported pincer complex of the isoelectronic telluronium cation the σ interaction is in an opposite direction, *i.e.*, it has a M → L character, thus classifying telluronium as a Z-type ligand.[30] This difference in σ-bonding characteristics between sulfonium and telluronium can be rationalized by the so-called inert-pair effect,[31] which in this case reflects the difference in energy of the 3s electrons of sulfonium compared to the 5s

Open Access Article. Published on 14 March 2022. Downloaded on 2/9/2026 9:09:14 AM.
This article is licensed under a Creative Commons Attribution 3.0 Unported Licence.

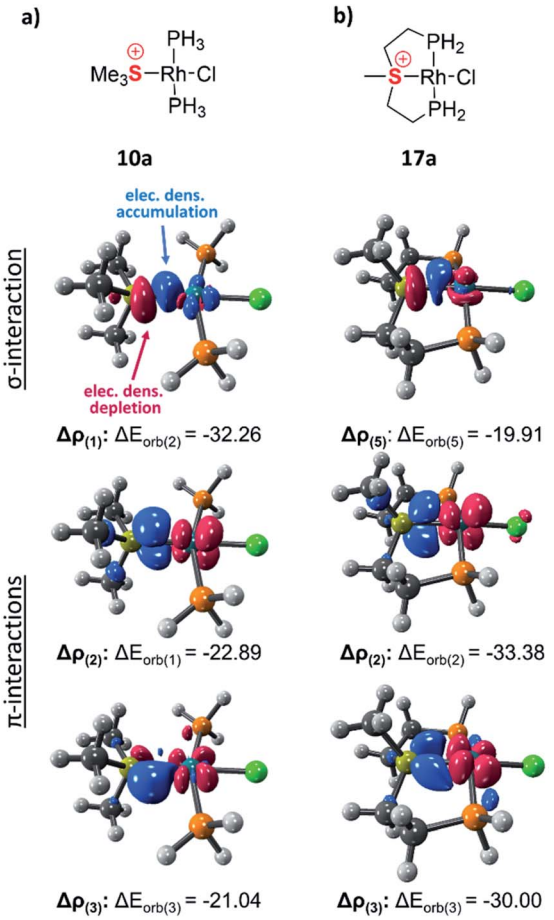

Fig. 5 Selected deformation density plots of model complexes **10a** (a) and **17a** (b) (all energies are given in kcal mol^{-1}).

electrons in telluronium. In the latter the energy of this lone pair is too low to play any role in the bonding to the metal; this can only occur thanks to the donation from the metal's d orbital to the σ* orbitals of telluronium. Therefore, while isoelectronic, sulfonium and telluronium systems are not isolobal.

As evident from Table 2 in terms of their BDEs and σ-donation, sulfonium cations are nearly similar to sulfides and sulfoxides. However, sulfonium cations are significantly stronger π-acceptors, with π-back-bonding interaction being predominant. This is quite unusual and not the case even for the strongly π-acidic perfluorinated phosphines (in complexes **14a–c**), where similarly to common phosphines (in **13a** and **13b**), σ-donation still prevails. This predominance of π-back-donation over σ-donation appears specific only to cationic ligands considered here. Compared to the latter, the π-acidity of sulfonium stands between that of N-heterocyclic nitrenium ([NHN]$^+$, in **15a**) and N-heterocyclic phosphenium ([NHP]$^+$, in **15b**), and is comparable to Alcarazo's tris-cationic phosphine PR^{3+} (in **15c**).[32]

With the cationic [PtMe]$^+$ fragment the calculations confirmed that the monodentate sulfonium complexes **16a** and **16b** (Table 2) are kinetically stable, despite the electrostatic repulsion between the positively charged metal fragment and

Table 2 EDA-NOCV data for the monodentate [L(PH$_3$)$_2$MX]$^{n+}$ complexes

MX	RhCl										PtMe$^+$	
Ligand types	Sulfonium cations		Sulfides		Sulfoxides		Phosphines		Cationic ligands		Sulfonium cations	
Model complexes	**10a**	**10b**	**11a**	**11b**	**12a**	**12b**	**13a**	**13b**	**15b**	**15c**	**16a**	**16b**
L	SMe_3^+	SPh_3^+	SMe_2	SPh_2	DMSO	Ph_2SO	PMe_3	PPh_3		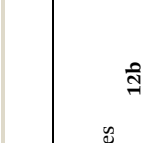	SMe_3^+	SPh_3^+
BDE	−38.57	−36.96	−36.21	−38.19	−39.80	−44.55	−70.06	−57.77				
σ-Bonding (% of σ/ΔE_{orb})	−32.26 (37.3%)	−31.13 (31.0%)	−35.03 (63.5%)	−34.39 (61.0%)	−39.82 (57.1%)	−40.73 (53.5%)	−56.69 (67.3%)	−53.31 (63.3%)				
π-Backbonding^a (% of π/ΔE_{orb})	−43.93 (50.8%)	−39.40 (39.2%)	−14.89 (27.0%)	−16.10 (28.6%)	−24.42 (35.0%)	−27.55 (38.0%)	−22.06 (26.2%)	−24.19 (28.7%)				

MX	RhCl						PtMe$^+$	
Ligand type	Perfluorinated phosphines			Cationic ligands			Sulfonium cations	
Model complex	**14a**	**14b**	**14c**	**15a**	**15b**	**15c**	**16a**	**16b**
L	PF_3	$P(CF_3)_3$	$P(C_6F_5)_3$	[NHN]$^+$	[NHP]$^+$	[PR$_3$]$^{3+}$	SMe_3^+	SPh_3^+
BDE^a	−56.76	−53.16	−51.35	−30.55	−57.57	−53.16	+48.60	+30.66
σ-Bonding^a (% of σ/ΔE_{orb})	−51.83 (51.4%)	−46.89 (49.7%)	−47.79 (55.1%)	−25.30 (40.3%)	−42.93 (44.3%)	−44.43 (42.6%)	−33.74 (57.3%)	−32.84 (56.9%)
π-Backbonding^{a,b} (% of π/ΔE_{orb})	−44.61 (43.3%)	−40.75 (43.2%)	−32.21 (37.1%)	−29.19 (46.4%)	−62.42 (52.3%)	−46.17 (44.2%)	−17.20 (29.2%)	−13.53 (23.5%)

^{a} All energies are given in kcal mol^{-1}. ^{b} Sum of the ⊥ and ∥ π-interactions.

© 2022 The Author(s). Published by the Royal Society of Chemistry

Open Access Article. Published on 14 March 2022. Downloaded on 2/9/2026 9:09:14 AM.
This article is licensed under a Creative Commons Attribution 3.0 Unported Licence.

Table 3 EDA-NOCV data for the $[LMX]^{n+}$ sulfonium pincer complexes

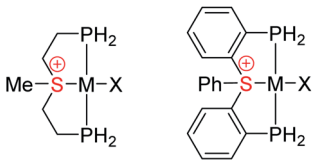

17a, 18a 17b, 18b

MX	RhCl		$PtMe^+$	
Model complex	**17a**	**17b**	**18a**	**18b**
σ-Bonding[a]	−19.91	−18.17	−47.16	−45.02
π-Back bonding[a,b]	−63.38	−59.10	−39.72	−41.57

[a] All energies are given in kcal mol^{-1}. [b] Sum of the ⊥ and ∥ π-interactions.

the sulfonium ligand responsible for the calculated positive BDE values. The obtained density plots of the model Pt complexes **16a** and **16b** were comparable in shape with those of the Rh complexes **10a** and **10b** (Fig. S18†), with prominent σ- and π-symmetric interactions. As expected for a positively charged metal center, the contribution of the π back-bonding in these model Pt complexes is significantly weaker than in their RhCl counterparts, yet still not negligible.

The influence of the pincer framework on bonding in both the Rh complexes **17a** and **17b** and their Pt analogues **18a** and **18b** is quite pronounced. As evident from Table 3, one can see that in both complexes the geometry deformations imposed by the pincer ligands strengthen the π back-donation within the complexes, so that the overall π/σ ratio significantly increases. Remarkably, in the case of the Pt complexes **18a** and **18b** π back-bonding even becomes comparable to the σ-donation, in spite of the positive charge on the metal center.

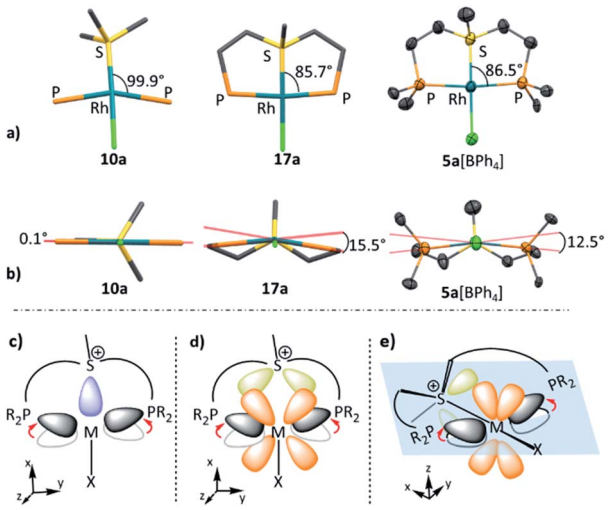

Fig. 6 The in-plane (a) and out-of-plane (b) deformations in model complexes **10a**, **17a** and **5a**[BPh_4] (hydrogen atoms, BPh_4 counter anion, and phenyl rings are omitted for clarity); schematic representation effect of pincer framework induced the in-plane and out-of-plane deformations on the σ (c) and π-interactions (d and e).

Table 4 Comparison of the σ and π interaction energies in model complexes **10a** and **10b**, **17a** and **17b**, **16a** and **16b**, and **18a** and **18b**[a]

Model complex		ΔE_{orb} of L → M σ-Donation[b]	ΔE_{orb} of ∥ M → L π-Backdonation[b]	ΔE_{orb} of ⊥ M → L π-Backdonation[b]
Rh–Cl	**10a**	−32.26	−21.04	−22.89
	10b	−31.13	−18.10	−21.30
	17a	−19.91	−30.00	−33.38
	17b	−18.17	−30.02	−29.08
Pt–Me	**16a**	−33.74	−8.62	−8.58
	16b	−32.84	−6.42	−7.11
	18a	−47.16	−17.55	−22.17
	18b	−45.02	−22.70	−18.87

[a] For the corresponding deformation density plots, see Tables S22 and S23. [b] All energies are given in kcal mol^{-1}.

These changes in bonding character can be rationalized by comparing the geometries of the pincer complexes relative to the monodentate ones. The following discussion of the aliphatic and aromatic Rh complexes, as displayed in Fig. 6a, b and S19,† respectively, is also applicable to the Pt systems.

In the aliphatic sulfonium pincer systems (both **5a**[BPh_4] and its model analog **17a**), the average P–Rh–S angles are ∼15° smaller than in the optimized monodentate complex **10a** (Fig. 6a). Such a decrease essentially pushes the phosphine lone pairs closer to those of sulfonium, increasing repulsive interactions between them. Thus, the sulfonium lone-pair is pushed away from the metal, which results in weakening the σ-donation in pincer complexes (Table 4, column 2). At the same time, this angle reduction also causes a stronger repulsion between the lone pairs of the phosphines and the filled d_{xy} orbital of the metal, shifting electron density closer to the adjacent σ*-orbital of the sulfonium (Fig. 6b). An enhanced in-plane π-back-donation is thus induced (Table 4, column 3).

In addition, the pincer framework also distorts the otherwise nearly planar coordination environment around the metal, pushing the two phosphines out of the coordination plane (Fig. 6b). This in turn results in repulsive interactions with the filled d_{xz} orbital, similarly strengthening the interaction with the perpendicular σ*-orbital of the sulfonium (Fig. 6c). Therefore, π-back-donation in the perpendicular plane increases as well (Table 4, column 4).

Overall, the EDA-NOCV data clearly points out that geometric distortion imposed by the pincer framework not only preserves the unique characteristics of sulfonium cations as weak σ-donors and potent π-acceptors, but also enhances them. For comparison, an analogous attempt to incorporate a phosphenium moiety within a pincer framework resulted in a full charge transfer from the metal to the ligand, transforming it into a phosphide.[33]

Conclusions

To summarize, in this paper we have consolidated the status of sulfonium cations among the family of rare cationic ligands

© 2022 The Author(s). Published by the Royal Society of Chemistry

Open Access Article. Published on 14 March 2022. Downloaded on 2/9/2026 9:09:14 AM. This article is licensed under a Creative Commons Attribution 3.0 Unported Licence.

demonstrating for the first time that their coordination chemistry can be extended to the Pt group metals. We also prepared the very first examples of metal-coordinated aromatic sulfonium cations. These unusual compounds might represent stable analogs of possible transient intermediates forming during Pd-catalyzed cross-coupling of sulfonium salts. Our calculations suggested that sulfonium cations are among the best π-acceptors available. Moreover, the pincer frameworks which offer additional robustness also intensify this propensity. These scaffolds might therefore be the key to transform sulfonium complexes from a chemical curiosity into potential π-acid catalysts, the applications of which are currently studied in our lab.

Data availability

Experimental procedures, NMR spectra and computational details are given in ESI.†

Author contributions

Y. T. conceived the project, R. L., N. B., and O. C. performed the experiments, V. S. performed the XRD data refinement and DFT calculations, and V. S., Y. T., and F. T. wrote the paper.

Conflicts of interest

There are no conflicts of interest.

Acknowledgements

We would like to thank Prof. Chris H. Hendon and Mr Min-Chieh Yang from the University of Oregon, USA, and Dr Veniamin Borin from the Hebrew University for their valuable advice in our computational studies. R. L. expresses her gratitude for the CSC-HUJI fellowship. We thank Dr Roy Hoffman for his assistance in performing 2D ^{103}Rh and ^{195}Pt NMR measurements. Our deep gratitude is also given to our colleagues from the Hebrew University, Prof. Dmitri Gelman, Prof. Avi Bino and Prof. Silvio Biali, for their kind help and support throughout our research.

Notes and references

1 (*a*) A. F. Hill, G. R. Owen, A. J. P. White and D. J. Williams, *Angew. Chem., Int. Ed.*, 1999, **38**, 2759; (*b*) D. You and F. P. Gabbaï, *Trends Chem.*, 2019, **1**, 485–496; (*c*) A. Amgoune and D. Bourissou, *Chem. Commun.*, 2011, **47**, 859–871.

2 (*a*) J. Fajardo Jr and J. C. Peters, *Inorg. Chem.*, 2021, **60**, 1220–1227; (*b*) T. J. Del Castillo, N. B. Thompson and J. C. Peters, *J. Am. Chem. Soc.*, 2016, **138**, 5341–5350; (*c*) J. S. Anderson, J. Rittle and J. C. Peters, *Nature*, 2013, **501**, 84–87.

3 (*a*) L. J. Clouston, V. Bernales, R. K. Carlson, L. Gagliardi and C. C. Lu, *Inorg. Chem.*, 2015, **54**, 9263–9270; (*b*) J. Ye, R. C. Cammarota, J. Xie, M. V. Vollmer, D. G. Truhlar, C. J. Cramer, C. C. Lu and L. Gagliardi, *ACS Catal.*, 2018, **8**, 4955–4968; (*c*) B. J. Graziano, M. V. Vollmer and C. C. Lu, *Angew. Chem., Int. Ed.*, 2021, **60**, 15087–15094; (*d*) M. V. Vollmer, J. Ye, J. C. Linehan, B. J. Graziano, A. Preston, E. S. Wiedner and C. C. Lu, *ACS Catal.*, 2020, **10**, 2459–2470; (*e*) J. T. Moore and C. C. Lu, *J. Am. Chem. Soc.*, 2020, **142**, 11641–11646; (*f*) R. C. Cammarota, J. Xie, S. A. Burgess, M. V. Vollmer, K. D. Vogiatzis, J. Ye, J. C. Linehan, A. M. Appel, C. Hoffmann, X. Wang, V. G. Young and C. C. Lu, *Chem. Sci.*, 2019, **10**, 7029–7042.

4 (*a*) J. Takaya and N. Iwasawa, *J. Am. Chem. Soc.*, 2017, **139**, 6074–6077; (*b*) M. Devillard, R. Declercq, E. Nicolas, A. W. Ehlers, J. Backs, N. Saffon-Merceron, G. Bouhadir, J. C. Slootweg, W. Uhl and D. Bourissou, *J. Am. Chem. Soc.*, 2016, **138**, 4917–4926; (*c*) B. R. Barnett, C. E. Moore, A. L. Rheingold and J. S. Figueroa, *J. Am. Chem. Soc.*, 2014, **136**, 10262–10265.

5 (*a*) F. Inagaki, C. Matsumoto, Y. Okada, N. Maruyama and C. Mukai, *Angew. Chem., Int. Ed.*, 2015, **54**, 818–822; (*b*) A. Ueno, K. Watanabe, C. G. Daniliuc, G. Kehr and G. Erker, *Chem. Commun.*, 2019, **55**, 4367–4370; (*c*) F. Inagaki, K. Nakazawa, K. Maeda, T. Koseki and C. Mukai, *Organometallics*, 2017, **36**, 3005–3008; (*d*) R. Murakami, H. Tanishima, D. Naito, H. Kawamitsu, R. Kamo, A. Uchida, K. Kawasaki, C. Kiyohara, M. Matsuo, K. Maeda and F. Inagaki, *Tetrahedron Lett.*, 2021, **78**, 153267; (*e*) R. Murakami and F. Inagaki, *Tetrahedron Lett.*, 2019, **60**, 151231; (*f*) F. Inagaki, K. Maeda, K. Nakazawa and C. Mukai, *Eur. J. Org. Chem.*, 2018, **2018**, 2972–2976.

6 (*a*) H. Yang and F. P. Gabbai, *J. Am. Chem. Soc.*, 2015, **137**, 13425–13432; (*b*) D. You, H. Yang, S. Sen and F. P. Gabbaï, *J. Am. Chem. Soc.*, 2018, **140**, 9644–9651; (*c*) Y.-H. Lo and F. P. Gabbaï, *Angew. Chem., Int. Ed.*, 2019, **58**, 10194–10197; (*d*) D. You and F. P. Gabbaï, *J. Am. Chem. Soc.*, 2017, **139**, 6843–6846; (*e*) S. Sen, I.-S. Ke and F. P. Gabbaï, *Organometallics*, 2017, **36**, 4224–4230; (*f*) D. You, J. E. Smith, S. Sen and F. P. Gabbaï, *Organometallics*, 2020, **39**, 4169–4173; (*g*) R. R. Rodrigues and F. P. Gabbaï, *Molecules*, 2021, **26**, 1985; (*h*) J. S. Jones and F. P. Gabbai, *Chem.–Eur. J.*, 2017, **23**, 1136–1144.

7 (*a*) L. C. Wilkins, Y. Kim, E. D. Litle and F. P. Gabbaï, *Angew. Chem., Int. Ed.*, 2019, **58**, 18266–18270; (*b*) E. D. Litle, L. C. Wilkins and F. P. Gabbaï, *Chem. Sci.*, 2021, **12**, 3929.

8 (*a*) P. Redero, T. Hartung, J. Zhang, L. D. M. Nicholls, G. Zichen, M. Simon, C. Golz and M. Alcarazo, *Angew. Chem., Int. Ed.*, 2020, **59**, 23527; (*b*) T. Johannsen, C. Golz and M. Alcarazo, *Angew. Chem., Int. Ed.*, 2020, **59**, 22779–22784; (*c*) K. Sprenger, C. Golz and M. Alcarazo, *Eur. J. Org. Chem.*, 2020, 6245–6254; (*d*) J. Zhang, M. Simon, C. Golz and M. Alcarazo, *Angew. Chem., Int. Ed.*, 2020, **59**, 5647–5650; (*e*) T. Hartung, R. Machleid, M. Simon, C. Golz and M. Alcarazo, *Angew. Chem., Int. Ed.*, 2020, **59**, 5660–5664; (*f*) L. D. M. Nicholls and M. Alcarazo, *Chem. Lett.*, 2019, **48**, 1; (*g*) H. Tinnermann, L. D. M. Nicholls, T. Johannsen, C. Wille, C. Golz, R. Goddard and M. Alcarazo, *ACS Catal.*, 2018, **8**, 10457–10463; (*h*) L. D. M. Nicholls, M. Marx, T. Hartung, E. González-Fernández, C. Golz and M. Alcarazo, *ACS Catal.*, 2018, **8**, 6079–6085; (*i*) L. Gu,

© 2022 The Author(s). Published by the Royal Society of Chemistry

Open Access Article. Published on 14 March 2022. Downloaded on 2/9/2026 9:09:14 AM. This article is licensed under a Creative Commons Attribution 3.0 Unported Licence.

L. M. Wolf, A. Zieliński, W. Thiel and M. Alcarazo, *J. Am. Chem. Soc.*, 2017, **139**, 4948–4953; (*j*) E. González-Fernández, L. D. M. Nicholls, L. D. Schaaf, C. Farès, C. W. Lehmann and M. Alcarazo, *J. Am. Chem. Soc.*, 2017, **139**, 1428–1431; (*k*) G. Mehler, P. Linowski, J. Carreras, A. Zanardi, J. W. Dube and M. Alcarazo, *Chem.–Eur. J.*, 2016, **22**, 15320–15327; (*l*) M. Alcarazo, *Acc. Chem. Res.*, 2016, **49**, 1797–1805; (*m*) E. Haldón, A. Kozma, H. Tinnermann, L. Gu, R. Goddard and M. Alcarazo, *Dalton Trans.*, 2016, **45**, 1872–1876; (*n*) H. Tinnermann, C. Wille and M. Alcarazo, *Angew. Chem., Int. Ed.*, 2014, **53**, 8732–8736; (*o*) M. Alcarazo, *Chem.–Eur. J.*, 2014, **20**, 7868–7877; (*p*) A. Kozma, T. Deden, J. Carreras, C. Wille, J. Petuškova, J. Rust and M. Alcarazo, *Chem.–Eur. J.*, 2014, **20**, 2208–2214; (*q*) J. Carreras, G. Gopakumar, L. Gu, A. Gimeno, P. Linowski, J. Petuškova, W. Thiel and M. Alcarazo, *J. Am. Chem. Soc.*, 2013, **135**, 18815–18823; (*r*) J. Carreras, M. Patil, W. Thiel and M. Alcarazo, *J. Am. Chem. Soc.*, 2012, **134**, 16753–16758.

9 J. W. Dube, Y. Zheng, W. Thiel and M. Alcarazo, *J. Am. Chem. Soc.*, 2016, **138**, 6869–6877.

10 (*a*) S. I. Kozhushkov and M. Alcarazo, *Eur. J. Inorg. Chem.*, 2020, **2020**, 2486–2500; (*b*) D. Kaiser, I. Klose, R. Oost, J. Neuhaus and N. Maulide, *Chem. Rev.*, 2019, **119**, 8701–8780; (*c*) V. G. Nenaidenko and E. S. Balenkova, *Russ. J. Org. Chem.*, 2003, **39**, 291–330; (*d*) L.-Q. Lu, T.-R. Li, Q. Wang and W.-J. Xiao, *Chem. Soc. Rev.*, 2017, **46**, 4135–4149; (*e*) V. K. Aggarwal and C. L. Winn, *Acc. Chem. Res.*, 2004, **37**, 611–620; (*f*) D. Kaiser, I. Klose, R. Oost, J. Neuhaus and N. Maulide, *Chem. Rev.*, 2019, **119**, 8701–8780; (*g*) A. C. B. Burtoloso, R. M. P. Dias and I. A. Leonarczyk, *Eur. J. Org. Chem.*, 2013, **2013**, 5005–5016.

11 (*a*) J. Srogl, G. D. Allred and L. S. Liebeskind, *J. Am. Chem. Soc.*, 1997, **119**, 12376–12377; (*b*) F. Berger, M. B. Plutschack, J. Riegger, W. Yu, S. Speicher, M. Ho, N. Frank and T. Ritter, *Nature*, 2019, **567**, 223–228; (*c*) J. Li, J. Chen, R. Sang, W.-S. Ham, M. B. Plutschack, F. Berger, S. Chabbra, A. Schnegg, C. Genicot and T. Ritter, *Nat. Chem.*, 2020, **12**, 56; (*d*) P. Cowper, Y. Jin, M. D. Turton, G. Kociok-Köhn and S. E. Lewis, *Angew. Chem., Int. Ed.*, 2016, **55**, 2564–2568; (*e*) P. S. Engl, A. P. Häring, F. Berger, G. Berger, A. Pérez-Bitrián and T. Ritter, *J. Am. Chem. Soc.*, 2019, **141**, 13346–13351; (*f*) H. Jia, A. P. Häring, F. Berger, L. Zhang and T. Ritter, *J. Am. Chem. Soc.*, 2021, **143**, 7623–7628; (*g*) E. M. Alvarez, T. Karl, F. Berger, L. Torkowski and T. Ritter, *Angew. Chem., Int. Ed.*, 2021, **60**, 13609–13613; (*h*) J. T. Chen, J. K. Li, M. B. Plutschack, F. Berger and T. Ritter, *Angew. Chem., Int. Ed.*, 2020, **59**, 5616–5620; (*i*) F. Ye, F. Berger, H. Jia, J. Ford, A. Wortman, J. Börgel, C. Genicot and T. Ritter, *Angew. Chem., Int. Ed.*, 2019, **58**, 14615–14619; (*j*) S.-M. Wang, H.-X. Song, X.-Y. Wang, N. Liu, H.-L. Qin and C.-P. Zhang, *Chem. Commun.*, 2016, **52**, 11893–11896; (*k*) S.-M. Wang, X.-Y. Wang, H.-L. Qin and C.-P. Zhang, *Chem.–Eur. J.*, 2016, **22**, 6542–6546; (*l*) Z.-Y. Tian, S.-M. Wang, S.-J. Jia, H.-X. Song and C.-P. Zhang, *Org. Lett.*, 2017, **19**, 5454–5457; (*m*) Z.-Y. Tian and C.-P. Zhang, *Chem. Commun.*, 2019, **55**, 11936–11939; (*n*) H. Minami, K. Nogi and H. Yorimitsu, *Org. Lett.*, 2019, **21**, 2518–2522; (*o*) H. Minami, S. Otsuka, K. Nogi and H. Yorimitsu, *ACS Catal.*, 2018, **8**, 579–583; (*p*) D. C. Simkó, P. Elekes, V. Pázmándi and Z. Novák, *Org. Lett.*, 2018, **20**, 676–679.

12 (*a*) J. V. Crivello, *J. Polym. Sci., Part A: Polym. Chem.*, 1999, **37**, 4241–4254; (*b*) Y. Takahashi, S. Kodama and Y. Ishii, *Organometallics*, 2018, **37**, 1649–1651; (*c*) C. O. Yanez, C. D. Andrade and K. D. Belfield, *Chem. Commun.*, 2009, 827–829.

13 (*a*) A. Péter, G. J. P. Perry and D. J. Procter, *Adv. Synth. Catal.*, 2020, **362**, 2135–2142; (*b*) X. Wang, L. Truesdale and J. Q. Yu, *J. Am. Chem. Soc.*, 2010, **132**, 3648–3649; (*c*) X.-G. Zhang, H.-X. Dai, M. Wasa and J.-Q. Yu, *J. Am. Chem. Soc.*, 2012, **134**, 11948–11951; (*d*) L.-S. Zhang, K. Chen, G.-H. Chen, B.-J. Li, S. Luo, Q.-Y. Guo, J.-B. Wei and Z.-J. Shi, *Org. Lett.*, 2013, **15**, 10–13.

14 (*a*) Y. Kim, M. Kim and F. P. Gabbaï, *Org. Lett.*, 2010, **12**, 600–602; (*b*) H. Zhao and F. P. Gabbai, *Org. Lett.*, 2011, **13**, 1444; (*c*) F. A. Tsao, A. E. Waked, L. Cao, J. Hofmann, L. Liu, S. Grimme and D. W. Stephan, *Chem. Commun.*, 2016, **52**, 12418–12421.

15 (*a*) H. Zhao and F. P. Gabbaï, *Nat. Chem.*, 2010, **2**, 984–990; (*b*) Y. Kim, H. Zhao and F. P. Gabbaï, *Angew. Chem., Int. Ed.*, 2009, **48**, 4957–4960.

16 (*a*) R. D. Adams and D. F. Chodosh, *J. Organomet. Chem.*, 1976, **120**, C39; (*b*) R. D. Adams and D. F. Chodosh, *J. Am. Chem. Soc.*, 1978, **100**, 812–817; (*c*) R. D. Adams and M. Shiralian, *Organometallics*, 1982, **1**, 883; (*d*) R. D. Adams, C. Blankenship, B. E. Segmueller and M. Shiralian, *J. Am. Chem. Soc.*, 1983, **105**, 4319–4326; (*e*) T. Yoshida, T. Adachi, K. Sato, K. Baba and T. Kanokogi, *J. Chem. Soc., Chem. Commun.*, 1993, 1511–1513.

17 P. B. Kettler, *Org. Process Res. Dev.*, 2003, **7**, 342–354.

18 (*a*) M. Albrecht and G. Van Koten, *Angew. Chem., Int. Ed.*, 2001, **40**, 3750–3781; (*b*) E. Peris and R. H. Crabtree, *Chem. Soc. Rev.*, 2018, **47**, 1959–1968.

19 (*a*) Y. Tulchinsky, M. A. Iron, M. Botoshansky and M. Gandelman, *Nat. Chem.*, 2011, **3**, 525–531; (*b*) Y. Tulchinsky, S. Kozuch, P. Saha, M. Botoshansky, L. Shimon and M. Gandelman, *Chem. Sci.*, 2014, **5**, 1305.

20 (*a*) C. Huang, J. Feng, R. Ma, S. Fang, T. Lu, W. Tang, D. Du and J. Gao, *Org. Lett.*, 2019, **21**, 9688–9692; (*b*) C. O. Yanez, C. D. Andrade and K. D. Belfield, *Chem. Commun.*, 2009, 827–829.

21 Searches were performed on the Cambridge Structural Database on Jan. 2022.

22 (*a*) G. J. Kubas and R. R. Ryan, *Inorg. Chim. Acta*, 1981, **47**, 131; (*b*) R. R. Ryan, P. G. Eller and G. J. Kubas, *Inorg. Chem.*, 1976, **15**, 797–799.

23 R. Meij, D. J. Stufkens and K. Vrieze, *J. Organomet. Chem.*, 1979, **164**, 353–370.

24 (*a*) D. L. M. Suess and J. C. Peters, *Organometallics*, 2012, **31**, 5213–5222; (*b*) F. Meyer, E. Hupf, E. Lork, S. Grabowsky, S. Mebs and J. Beckmann, *Eur. J. Inorg. Chem.*, 2020, 3829–3836.

Open Access Article. Published on 14 March 2022. Downloaded on 2/9/2026 9:09:14 AM.
This article is licensed under a Creative Commons Attribution 3.0 Unported Licence.

25 A. Kozma, J. Petuskova, C. W. Lehmann and M. Alcarazo, *Chem. Commun.*, 2013, **49**, 4145.
26 A. Vigalok, L. J. W. Shimon and D. Milstein, *J. Am. Chem. Soc.*, 1998, **120**, 477–483.
27 (*a*) T. Ziegler and A. Rauk, *Inorg. Chem.*, 1979, **18**, 1755; (*b*) T. Ziegler and A. Rauk, *Theor. Chim. Acta*, 1977, **46**, 1.
28 (*a*) A. Michalak, M. Mitoraj and T. Ziegler, *J. Phys. Chem. A*, 2008, **112**, 1933–1939; (*b*) M. Mitoraj and A. Michalak, *Organometallics*, 2007, **26**, 6576–6580; (*c*) M. Mitoraj and A. Michalak, *J. Mol. Model.*, 2007, **13**, 347–355; (*d*) M. Mitoraj and A. Michalak, *J. Mol. Model.*, 2008, **14**, 681–687; (*e*) M. Mitoraj, H. Zhu, A. Michalak and T. Ziegler, *Int. J. Quantum Chem.*, 2009, **109**, 3379–3386.
29 (*a*) M. Mitoraj and A. Michalak, *Organometallics*, 2007, **26**, 6576–6580; (*b*) M. Mitoraj and A. Michalak, *J. Mol. Model.*, 2007, **13**, 347–355.
30 (*a*) T.-P. Lin and F. P. Gabbaï, *J. Am. Chem. Soc.*, 2012, **134**, 12230–12238; (*b*) T. P. Lin and F. P. Gabbaï, *Angew. Chem., Int. Ed.*, 2013, **52**, 3864–3868.
31 T. Overton, J. Rourke, M. Weller, F. Amstrong and P. Atkins, *Inorganic Chemistry*, Oxford University Press, 5th edn, New York, 2010, p. 267.
32 J. Petuskova, M. Patil, S. Holle, C. W. Lehmann, W. Thiel and M. Alcarazo, *J. Am. Chem. Soc.*, 2011, **133**, 20758.
33 B. Pan, Z. Xu, M. W. Bezpalko, B. M. Foxman and C. M. Thomas, *Inorg. Chem.*, 2012, **51**, 4170–4179.

© 2022 The Author(s). Published by the Royal Society of Chemistry